Supporting Information

Autocatalytic Surface Explosion Chemistry of 2D Metal-Organic Frameworks

Christian Wäckerlin,[†,] and Karl-Heinz Ernst[†,‡,§,]**

† Surface Science and Coating Technologies, Empa - Swiss Federal Laboratories for Materials Research and Technology, Überlandstrasse 129, CH-8600 Dübendorf, Switzerland, E-mail: christian.waeckerlin@empa.ch, karl-heinz.ernst@empa.ch

‡ Department of Chemistry, University of Zurich, Winterthurerstrasse 190, CH-8057 Zürich, Switzerland

§ Nanosurf Laboratory, Institute of Physics, The Czech Academy of Sciences, Cukrovarnická 10, 162 00 Prague, Czech Republic

Contents

Detailed Experimental Methods

XPS was measured using non-monochromatized Al K_α X-rays, except for Fe $2p_{3/2}$ where Mg K_α X-rays were used because of overlap with Auger peaks from the copper substrate. The binding energy scale was calibrated on the Cu $2p_{3/2}$ peak (932.7 eV) and the Fermi level (0.0 eV). The intensities were normalized with respect to the Cu $2p_{3/2}$ signal and background spectra obtained on the clean samples were subtracted. STM images (Specs Aarhus 150) were recorded at room temperature in constant current mode with a mechanically cut and in-situ argon-ion etched Pt/Ir (90% Pt) tip. TPRS data were obtained using a quadrupole mass spectrometer. A special housing (Feulner cup) with a pinhole was installed to avoid collecting material from the sample holder.

The Cu(100) single crystal was prepared *via* consecutive Ar^+ ion sputtering and annealing cycles. SqA (3,4-Dihydroxy-3-cyclobutene-1,2-dione, Sigma Aldrich, purity 99%) was deposited by sublimation (T_{sub} = 493 K). Fe and Ni atoms were supplied by electron beam evaporators. Expect in case of the low coverages shown in Figure 3a, a multilayer (3 – 5 ML) of SqA was deposited onto the sample kept at room temperature, followed by deposition of Ni or Fe. The samples were then annealed for 5 min at the indicated temperatures.

M 2p Binding Energies and Quantification

In XPS, the M $2p_{3/2}$ binding energy does not only depend on the oxidation state of the ion but also on the character of the metal-ligand bond: more ionic ligand-metal bonds result in a decreased shielding of the metal and thus increased M 2p binding energies.[1] Indeed, the Fe $2p_{3/2}$ binding energy of FeSq (710.2 eV) is higher than those of Fe(II) species like FeO (708.4 eV)[2], Fe-phthalocyanine (708 eV),[3] but consistent with more ionic Fe(II) species such as $FeCl_2$ (709.8 eV)[1] or siderite ($FeCO_3$, 709.8 eV).[2] In view of the binding energy of Fe_2O_3 (709.8 eV),[1] a Fe(III) state cannot be excluded. NiSq shows the same trend: the Ni $2p_{3/2}$ binding energy of NiSq (854.8 eV) is

quite high compared to Ni(II)O (853.7 eV)[2] and closer to Ni(II) in more ionic compounds like $Ni(OH)_2$ (854.9 eV).[2] Because the binding energy of Ni(III) species Ni_2O_3 is already 855.8 eV,[4] a Ni(III) state can be excluded. Because the coordination motifs seen in the STM data evidence M(II)squarate complexes (Figure 2), M(III) complexes are excluded in both the Ni and Fe cases.

The quantifications were performed using the photoelectron cross sections from ref. 5 for Al Kα X-rays. Table S1 shows C/O and {Ni,Fe}/O stoichiometry determined by XPS.

The attenuation of the Cu 2p signal of the substrate was calculated as follows: We estimate an additional thickness of the Sq layer with respect to the O-(2√2×√2)R45° structure on Cu(100) of d = 0.3 nm. The inelastic electron mean free path at a kinetic energy of 557 eV (Cu $2p_{3/2}$ using Al Kα X-rays) from the universal curve[6] is λ =1.25 nm. Thus the Cu2p signal is attenuated to exp(−d/λ) = 79%.

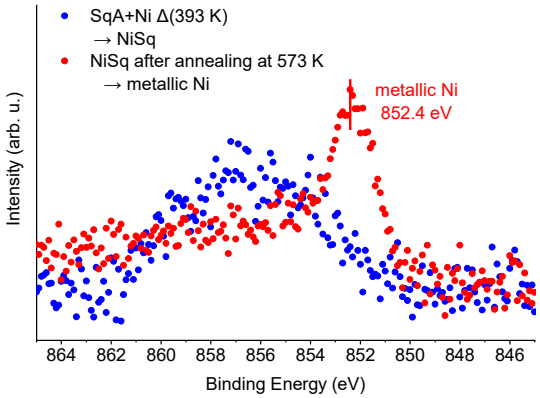

Figure S1. Ni $2p_{3/2}$ XP spectra of NiSq before and after annealing to 573 K.

Table S1. C/O and M/O stoichiometry determined by XPS

Sample	C/O stoichiometry
ideal	1.00
multilayer SqA	1.06
CuSq	1.07
NiSq	1.14
FeSq	1.20

Sample	M/O stoichiometry	Sq molecules / M atom
ideal 100% MSq	$\frac{1}{4\times8} = 0.03125$	8
FeSq high Fe dose	0.026	9.6
FeSq low Fe dose	0.008	29.7
NiSq	0.0165	15.1

Rate Equation Model

The rate equations 1 are numerically evaluated using 10000 time steps. r is the rate, $\nu = 10^{13}$ Hz the attempt frequency, R is the gas constant and $\theta_{CuSq}, \theta_{NiSq}, \theta_{FeSq}$ are the coverages of CuSq, NiSq and FeSq complexes. $\theta_* = 1 - \theta_{CuSq} - \theta_{NiSq} - \theta_{FeSq}$ is the coverage of vacancies. E_A^{CuSq} E_A^{NiSq-S}, E_A^{FeSq-S}, E_A^{NiSq-U} and E_A^{FeSq-U}, are activation energies (Table S2). The temperature T is increased at a rate of 1 K/s.

$$r(t) = -\frac{d\theta_{CuSq}}{dt} - \frac{d\theta_{FeSq}}{dt} - \frac{d\theta_{NiSq}}{dt}$$

$$\frac{d\theta_{CuSq}}{dt} = -\nu\,\theta_{CuSq}\exp\left[-\frac{E_A^{CuSq}}{RT}\right]$$

$$\frac{d\theta_{NiSq}}{dt} = -\nu\,\theta_*\theta_{NiSq}\exp\left[-\frac{E_A^{NiSq-U}}{RT}\right] - \nu\,\theta_{NiSq}\exp\left[-\frac{E_A^{NiSq-S}}{RT}\right]$$

$$\frac{d\theta_{FeSq}}{dt} = -\nu\,\theta_*\theta_{FeSq}\exp\left[-\frac{E_A^{FeSq-U}}{RT}\right] - \nu\,\theta_{FeSq}\exp\left[-\frac{E_A^{FeSq-S}}{RT}\right]$$

(Eqs. 1)

CuSq decomposes regularly (*i.e.* first order kinetics) with activation energy EA_{CuSq}. NiSq and FeSq have two modes of decomposition each: i) regular (blue) with higher activation energies

(E_A^{NiSq-S}, E_A^{FeSq-S}, "S" for stable) and ii) autocatalytic (red) with lower activation energies (E_A^{NiSq-U} and E_A^{FeSq-U}, "U" for unstable). Because the coverage of vacancies θ_* is initially zero, at first only the regular terms contribute. Once $\theta_* > 0$, the autocalytic decomposition sets in.

Table S2. Activation energies used to calculate the decomposition probabilities.

Parameter	***Value*** **(kJ/mol)**
$E_A{}^{CuSq}$	156
$E_A{}^{NiSq\text{-}S}$	122 + 30 = 152
$E_A{}^{NiSq\text{-}U}$	122
$E_A{}^{FeSq\text{-}S}$	136 + 30 = 166
$E_A{}^{FeSq\text{-}U}$	136

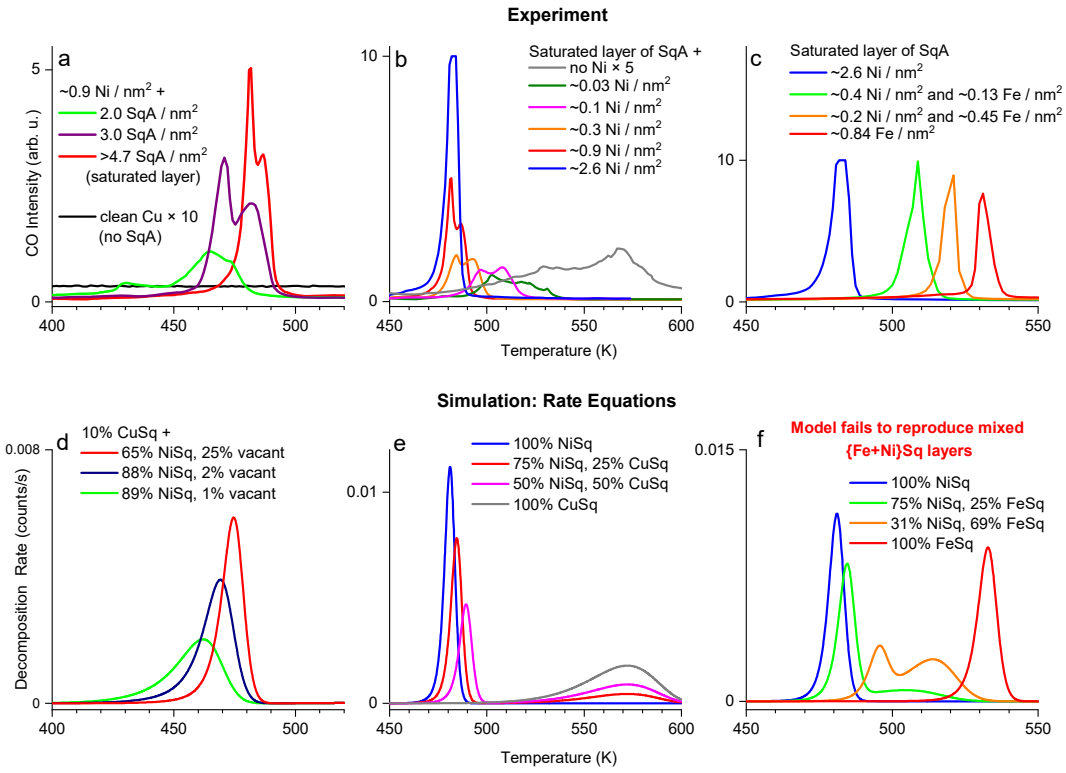

Figure S2. TPR simulations obtained by evaluation of the rate equation model (d-f) compared with the TPR data (a-c). The rate equation model reproduces the experimental data qualitatively, with the exception of mixed {Ni+Fe}Sq layers (c).

Spatial Model

Algorithm 1 is evaluated on a grid of 100 × 100 cells from 380 K to 650 K. The grid is initialized randomly with vacancies, Cu, Ni and Fe sites. The temperature is increased stepwise at a rate of 1 K/s. The number of vacant neighbors (*i.e.* not Ni, Fe or Cu) of every cell is evaluated by considering its 8 neighbor sites. To avoid edge effects, periodic boundary conditions are applied. The probabilities for decomposition p_X are calculated according to eqs. 2 with the activation energies E_A^X shown in Table S3. $\nu = 10^{13}$ Hz is the attempt frequency, $\Delta t = 0.01$ s is the duration of the time step and R is the gas constant.

Algorithm 1

```
for every timestep:
  for every cell:
    if cell is Cu:
      with probability p_Cu: set cell to vacant
    if cell is Ni:
      if number of neighboring vacant sites is less than 3:
         with probability p_Ni-U: set cell to vacant
      else
        with probability p_Ni-S: set cell to vacant
    if cell is Fe:
      if number of neighboring vacant sites is less than 3:
        with probability p_Fe-U: set cell to vacant
      else:
        with probability p_Fe-S: set cell to vacant
```

$$p_X = \nu \times \exp[-\frac{E_A^X}{RT}] \times \Delta t \quad \textbf{(Eqs. 2)}$$

If a Ni or Fe cell has 3 or more vacant neighbors it is considered "unstable" and decomposes with probabilities $p_{\{Ni,Fe\}\text{-}U}$ with the corresponding lower activation energies. Else, the cell is considered stable, decomposing with probabilities $p_{\{Ni,Fe\}\text{-}S}$ (see illustration in Figure S3).

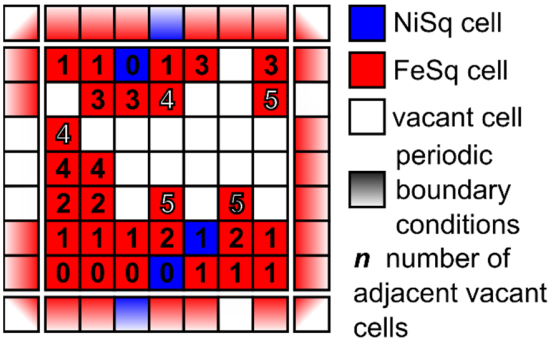

Figure S3: Illustration of the spatial model. The NiSq and FeSq cells with more than 3 adjacent vacant cells can decompose with a higher probability, i.e. lower activation energies in Eqs. 2. Periodic boundary conditions (shaded cells) are applied.

Table S3. Activation energies used to calculate the decomposition probabilities.

Rate equation	E_A **(kJ/mol)**
p_{Cu}	156
$p_{Ni\text{-}S}$	114 + 30 = 144
$p_{Ni\text{-}U}$	114
$p_{Fe\text{-}S}$	128 + 30 = 158
$p_{Fe\text{-}U}$	128

Notes on Both Models

For simplicity, the rate equation model and the spatial model are built up with the concepts and parameters. In case of CuSq, which decomposes in the rate equation model regularly (first order kinetics) and independent of the state of neighbors in the spatial model, both models yield identical results (Figure S4). This validates the implementation of the spatial model. For NiSq and FeSq, both species have regular modes of decomposition with $\Delta E = 30$ kJ/mol higher activation energies than the autocatalytic modes. In both models, the activation energies are tuned to match the experimental TPRS peak maxima of the pure CuSq, NiSq and FeSq layers. Because in the spatial model the decomposition fronts have to propagate through, the layers the activation energies for NiSq and FeSq are slightly lower in this model. The stabilization energy ΔE is tuned to reproduce the width of the TPRS peaks. The time steps are chosen sufficiently small such that even smaller values do not change the result.

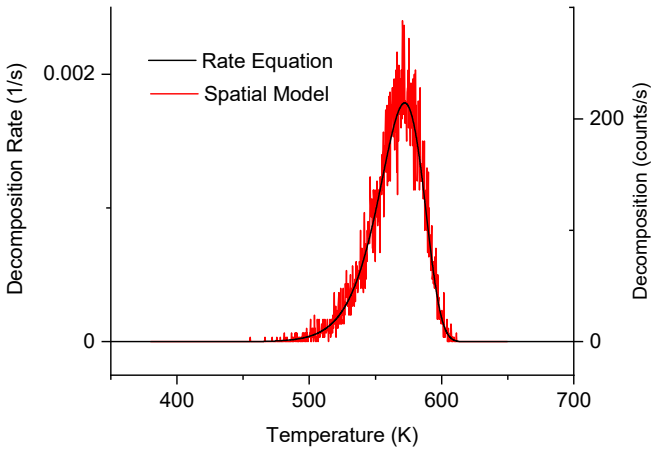

Figure S4. Decomposition rates of a 1 ML CuSq calculated with both models.

REFERENCES

(1) Grosvenor, A. P.; Kobe, B. A.; Biesinger, M. C.; McIntyre, N. S. Investigation of Multiplet Splitting of Fe 2p XPS Spectra and Bonding in Iron Compounds. *Surf. Interface Anal.* **2004**, *36*, 1564–1574.

(2) Biesinger, M. C.; Payne, B. P.; Grosvenor, A. P.; Lau, L. W. M.; Gerson, A. R.; Smart, R. St. C. Resolving Surface Chemical States in XPS Analysis of First Row Transition Metals, Oxides and Hydroxides: Cr, Mn, Fe, Co and Ni. *Appl. Surf. Sci.* **2011**, *257*, 2717–2730.

(3) Isvoranu, C.; Knudsen, J.; Ataman, E.; Schulte, K.; Wang, B.; Bocquet, M.-L.; Andersen, J. N.; Schnadt, J. Adsorption of Ammonia on Multilayer Iron Phthalocyanine. *J. Chem. Phys.* **2011**, *134*, 114711.

(4) Kim, K. S.; Winograd, N. X-Ray Photoelectron Spectroscopic Studies of Nickel-Oxygen Surfaces Using Oxygen and Argon Ion-Bombardment. *Surf. Sci.* **1974**, *43*, 625–643.

(5) Scofield, J. H. Hartree-Slater Subshell Photoionization Cross-Sections at 1254 and 1487 eV. *J. Electron Spectrosc. Relat. Phenom.* **1976**, *8*, 129–137.

(6) Seah, M. P.; Dench, W. A. Quantitative Electron Spectroscopy of Surfaces: A Standard Data Base for Electron Inelastic Mean Free Paths in Solids. *Surf. Interface Anal.* **1979**, *1*, 2–11.